Gauging Molecular Interactions between Substrates and Adsorbates. Substrate Mediation of Surface-Bound Chromophore Vibronic Coupling

L. Kelepouris,[†] Paweł Krysiński,[‡] and G. J. Blanchard*[,†]

Department of Chemistry, Michigan State University, East Lansing, Michigan 48824-1322, and Laboratory of Electrochemistry, Department of Chemistry, University of Warsaw, 02-093 Warsaw, Pasteura 1, Poland

Received: August 15, 2002; In Final Form: March 3, 2003

We have studied the steady-state and time-resolved optical response of substituted pyrene chromophores in solution and tethered to dielectric, doped semiconductor, and metallic substrates. The steady-state spectra of the substituted pyrenes indicate that both the $S_2 \leftarrow S_0$ and $S_1 \leftarrow S_0$ transitions play significant roles in the measured optical response. In solution, time-resolved measurements of the substituted pyrene chromophores reveal a zero-time anisotropy that depends on the identity of the substituent. We attribute this phenomenon to intramolecular interactions between the pyrene chromophore and the substituent. For chromophores bound to substrates, we find that there is no discernible motion on the nanosecond time scale and that the measured zero-time anisotropy depends on the identity of the substrate. The interactions between the chromophore and the substrate are manifested as the mediation of S_1-S_2 vibronic coupling in the chromophore.

Introduction

An area of great potential for interfacial materials science is the integration of biologically relevant molecules for use as sensing elements into well-organized, ultrathin layered structures. Success in this endeavor will require scientific and technological advances in several areas, including the creation of interfacial environments that can support biomolecules in their native state. We are interested in developing amphiphilic layered assemblies at electrochemically active interfaces so that we can realize the incorporation of biomolecules such as redox proteins and channel-forming proteins into layered interfaces for sensing applications.

We have demonstrated the ability to bind layered structures to electrochemically oxidized gold surfaces using covalent linking chemistry that was previously limited to growth on dielectric substrates.[1] This advance allows us to use a family of layered growth reactions for the creation of amphiphilic interfacial layers. We are also interested in using indium tin oxide (ITO) as a substrate material because of its combined electronic and optical properties, and the same chemistry used for growth on gold oxide surfaces can be used for ITO as well.[2] We need to characterize a series of interfacial structures on these substrates with an eye toward their local organization and dynamics. The extent to which the interfacial layers that we synthesize can mimic lipid bilayers will likely be a good indicator of their utility as nondenaturing supports for biomolecules. We report in this paper on our characterization of oxidized gold, ITO, and quartz substrates using tethered pyrene compounds as probes of local organization and dynamics.

We have chosen substituted pyrene derivatives as chromophores for this work (Figure 1) because we understand the optical properties of pyrene.[3] This chromophore exhibits "polarity"-dependent changes in its linear optical response that are mediated by dipolar coupling between its S_1 and S_2 excited states and the immediate environment. The $S_2 \leftarrow S_0$ and $S_1 \leftarrow S_0$ electronic transitions in pyrene are polarized nominally per-

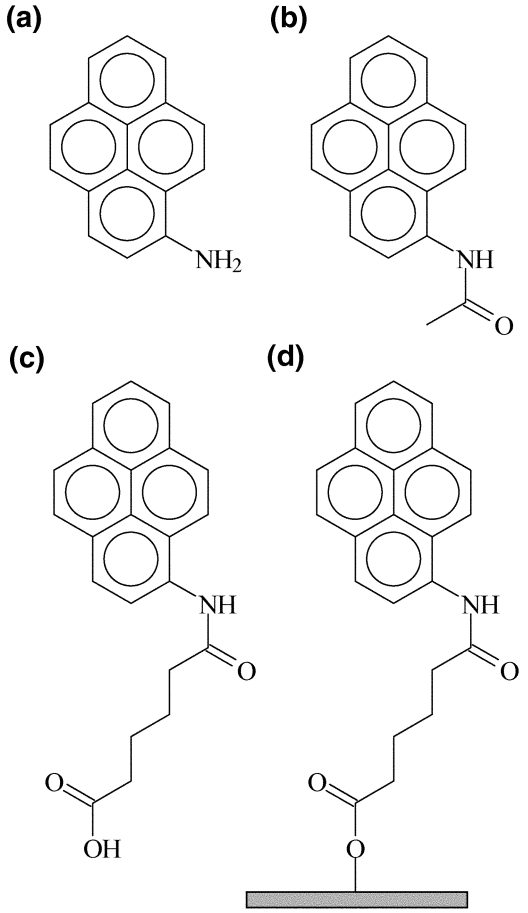

Figure 1. Structures of compounds used in this study: (a) 1-aminopyrene, (b) 1-acetamidopyrene, (c) 1-amidopyrene hexanoic acid, (d) 1-amidopyrene hexanoate bound to a substrate.

* To whom correspondence should be addressed. E-mail: blanchard@chemistry.msu.edu.
[†] Michigan State University.
[‡] University of Warsaw.

10.1021/jp026773m CCC: $25.00
Published on Web 04/05/2003

pendicular to one another, and the extent to which the local environment couples the coordinates spanned by b_{3g} vibrational modes determines the observed perturbation to the chromophore linear response. For substituted pyrene compounds, the presence of substituent(s) serves to break the symmetry of the chromophore, but the extent to which the excited electronic states are coupled is still determined to a significant extent by the chromophore local environment. We have observed that the local environment of several substituted pyrene derivatives mediates the optical response by altering the extent of vibronic coupling between the S_1 and S_2 manifolds (vide infra).

We have examined several interfacial systems using a substituted pyrene chromophore. Our experimental data show that the pyrene chromophore, present at the outermost extent of the interfacial layer structures that we form, does not exhibit measurable motional dynamics, at least over nanosecond time scales, and that there is substantial interaction between the pyrene chromophore and the substrate, as seen through changes in the vibronic coupling of excited states S_1 and S_2 of the tethered pyrene chromophore. We understand this effect in terms of dipole−induced dipole and induced dipole−induced dipole interactions. A comparison of time-resolved spectroscopic data for tethered pyrene at interfaces to data for the analogous species in solution (structures shown in Figure 1) reveals the importance of both intramolecular and intermolecular dipolar interactions in mediating vibronic coupling in these chromophores. Dielectric substrates appear to interact least strongly with the pyrene chromophores, with doped semiconductor and metallic substrates revealing substantially stronger couplings, as expected. The details of this interaction reveal that, for the gold- and ITO-bound chromophores, the pyrene π-plane must be oriented close to perpendicular to the substrate plane. This finding is consistent with the steady-state emission and IR absorption data for these systems. Taken collectively, our data demonstrate that the interfacial structures that we have developed will serve effectively as electrochemically active supports for biomolecules and that, when such systems are assembled, interactions between polar groups within the adsorbates and the substrate must be considered. This latter issue is often neglected in the design of molecular interfacial layers. Because the dominant interactions are thought to be the covalent or ionic bonds between the adlayer molecule headgroup and the substrate and between the layer constituent molecules, longer-range dipolar interactions between the substrate and functionalities incorporated into the adlayer and separated from the substrate are often neglected. However, there is growing experimental evidence that such interactions can be important and need to be taken into account.[4−8] It has been reported, for example, that cysteamine molecules self-assembled on gold surfaces adopt a predominantly gauche conformation because of the strong interactions of their amine terminal groups with the surface.[4,6] Similar effects have been seen for dipalmitoylphosphatidylethanolamine mercaptopropionamide[7] and cholesterylmercaptopropionamide,[8] a lipid molecule tethered to a gold surface through an amide linkage to mercaptopropionic acid.

Experimental Section

Chemicals. All chemicals used were of the highest quality available commercially: gold, gold-covered silicon, indium-doped tin oxide (ITO) on quartz (Delta Technologies, Ltd.), chromic acid (VWR Scientific Products), sulfuric acid (CCI, ACS/reagent grade), sodium sulfate (Spectrum Quality Products, Inc.), potassium chloride (Spectrum Chemical Mfg. Corp.), ferrocenemethanol (Aldrich, 97%), adipoyl chloride (Aldrich), 4-methylmorpholine (Aldrich, 99%), dry acetonitrile (Aldrich, 98%), chloroform (Aldrich, 99.8%), ethyl acetate (Spectrum Quality Products, Inc., ACS/reagent grade), *n*-dodecylamine (Aldrich, >99%), DPPE (1,3-dipalmitoyl-*sn*-glycero-3-phosphoethanolamine, Fluka, >99%), 1-aminopyrene (Fluka). Deionized water was available in-house.

Electrochemistry. Electrochemical measurements were made with a PC-controlled model 650A Electrochemical Workstation (CH Instruments, Austin, TX), using a small-volume three-electrode cell with a Pt wire counter electrode. All potentials are referenced to a Ag/AgCl/1 M KCl_{aq} reference electrode.

IRRAS Spectroscopy. For monolayers assembled on gold-plated silicon slides, infrared reflection−absorption spectra (IRRAS) were acquired with 4 cm^{-1} resolution (256 scans) using a Nicolet Magna 750 FTIR spectrometer equipped with an MCT type A detector. The external reflectance sample mount was set to an incidence angle of 80° with respect to the substrate normal.

Optical Ellipsometry. Ellipsometric thickness measurements of adlayers formed on the electrochemically oxidized gold surface were made with a Rudolph Auto-EL II optical ellipsometer operating at 632.8 nm. Rudolph DAFIBM software was used for data collection and processing.

Time-Resolved Emission Measurements. The time-correlated single-photon counting (TCSPC) system used to acquire lifetime and dynamical information has been described elsewhere,[9] and we recap its salient features here. The second harmonic of the output of a mode-locked CW Nd:YAG laser (Quantronix 416) is used to pump a cavity-dumped dye laser (Coherent 702-3) operated at 660 nm using Kiton Red laser dye (Exciton Chemical Co.). The output of the dye laser was typically 100-mW average power at a 4-MHz repetition rate with ~5-ps pulses. A fraction of each pulse is used as a temporal reference beam, with the remaining light being frequency doubled using a type I $LiIO_3$ crystal to provide 330-nm light for chromophore excitation. The polarization of the excitation beam is set to be vertical, and the emission polarization is selected using a Glan−Taylor prism. The system is operated in reverse time mode and is characterized by an instrument response function that is typically 30 ps fwhm.

Preparation of Gold Substrates and Oxide Layer Formation. Gold substrates for electrochemical measurements were 99.99% Au, 0.5-mm-diameter wires with tips melted to form gold-ball electrodes with an electrochemical area of 0.16 cm^2, as determined from cyclic voltammetry of $K_4Fe(CN)_6/K_3Fe(CN)_6$ in aqueous solution. The electrodes were cleaned by annealing in a reductive flame and then polarized cyclically (scan rate = 0.1 V/s) in the −0.3 to 1.5 V potential range in 0.5 M H_2SO_4(aq) solution. The electrodes were then cycled at the same rate in 0.5 M Na_2SO_4(aq) solution in the potential window of −0.5 to 1.2 V. Once reproducible voltammograms were obtained, the potential cycle was stopped at 1.2 V for 60 s, and under potential control, the electrodes were removed from the cell, washed with distilled water, and dried with a stream of nitrogen.

Planar gold substrates were made from silicon wafers, A = 2 cm^2, with evaporated gold (1000 Å) deposited on a chromium adhesion layer. The gold-coated substrates were cleaned by immersion in hot chromic acid (95 °C, 30 s) and rinsed with distilled water. The clean substrates were transferred to the electrochemical cell and polarized cyclically in 0.5 M Na_2SO_4(aq), to avoid dissolution of the chromium adhesion layer, with consequent delamination of the gold layer. This procedure

resulted in a stable open-circuit potential of the substrate of ca. 0.76 V, characteristic of the formation of a hydrated oxide layer on gold.

ITO Substrates. ITO-on-quartz substrates were cleaned first by brief immersion in hot chromic acid, followed by washing with distilled water. The substrates were refluxed for 5 min in an acetone/methanol solution (50:50, v/v), immersed into a solution of 1:1:5 (v/v/v) 30% H_2O_2/30% NH_4OH/H_2O for 5 min and agitated ultrasonically, and then soaked for 45 min at 60 °C in the same solution. Finally, they were rinsed with an abundance of water and dried thoroughly.

Adipate Adlayer Formation. Electrochemically oxidized gold and ITO substrates were reacted with adipoyl chloride in dry acetonitrile, using 4-methylmorpholine as a Lewis base (1: 50: 1, v/v/v) under nitrogen for ca. 12 h. The reacted substrates were removed from the reaction vessel and rinsed with ethyl acetate. Gold-plated silicon slides were then dried under a stream of nitrogen and used for IRRAS and ellipsometric measurements, giving a film thickness of 8.5 ± 1.5 Å, consistent with the addition of a monolayer of adipoyl chloride. Under ambient conditions, the acid chloride terminal functionalities were converted to carboxylic acids. The surface coverage was determined to be 1.5×10^{-10} mol cm^{-2}, evaluated electrochemically on gold-ball electrodes, using ferrocenemethanol covalently bonded to the adipate adlayer as the electrochemically active species. As discussed elsewhere, we believe that this measurement method yields a surface coverage value corresponding to less than a full monolayer for steric reasons.[1] The data that we present here point to significant aggregation of the pyrene chromophore on the surface, and this structural condition can potentially influence our measurement of surface reactive site density. In addition, the adipate adlayer upon which the electroactive component is bound is characterized by significant disorder (vide infra). This situation can lead to partial coverage of the surface by preventing some fraction of the terminal groups from being exposed for reaction with the electroactive species.

Results and Discussion

We are concerned with understanding the molecular-scale environment formed by the adlayers that we grow. These adlayers are composed of a chromophore-containing monolayer bound covalently to the adipate monolayer formed on the oxidized gold, ITO, or SiO_x substrate. We consider the growth of the monolayer before addressing the dynamics of the substituted pyrene chromophore(s).

Fluorophore Attachment and Anisotropy Measurements. The acid chloride terminal functionality on gold-plated silicon slides and ITO on quartz was reacted with 1-aminopyrene by exposing substrates covered with an adipoyl chloride adlayer to 10 mL of 0.5 mM 1-aminopyrene in dry acetonitrile with 0.1 mL of 4-methylmorpholine under nitrogen overnight. The substrates were then removed, washed with ethyl acetate, and dried. The resulting chromophore coverages were evaluated electrochemically[1] to be 5.6×10^{-12} mol cm^{-2} (Au surface) and 1.7×10^{-11} mol cm^{-2} (ITO surface), on the basis of its known electrochemistry.[10,11]

Steady-state spectroscopy on this system reveals the presence of excimers in the monolayers. We make this statement on the basis of a comparison of the steady-state emission spectra of the surface-bound species (Figure 2) with the solution-phase spectra of 1-acetamidopyrene (Figure 3).[12,13] The emission spectra of the chromophores bound to ITO (Figure 2a) and quartz (Figure 2b) show a broad, featureless maximum, centered near 420 nm for ITO and near 380 nm for quartz. For the ITO-bound pyrene, the emission band is qualitatively similar to the solution-phase excimer band for 1-amidopyrene hexanoic acid, and for quartz-bound pyrene, the emission maximum appears to lie closer to that of the solution-phase monomer species. The absence of resolved spectral features in the vicinity of the emission maximum for both of the surface-bound species is consistent with excimer formation, and there is substantial intensity to the red of the solution-phase monomer band, in a spectral region where pyrene aggregates are known to emit. The difference between the spectra shown in Figure 2a and b might

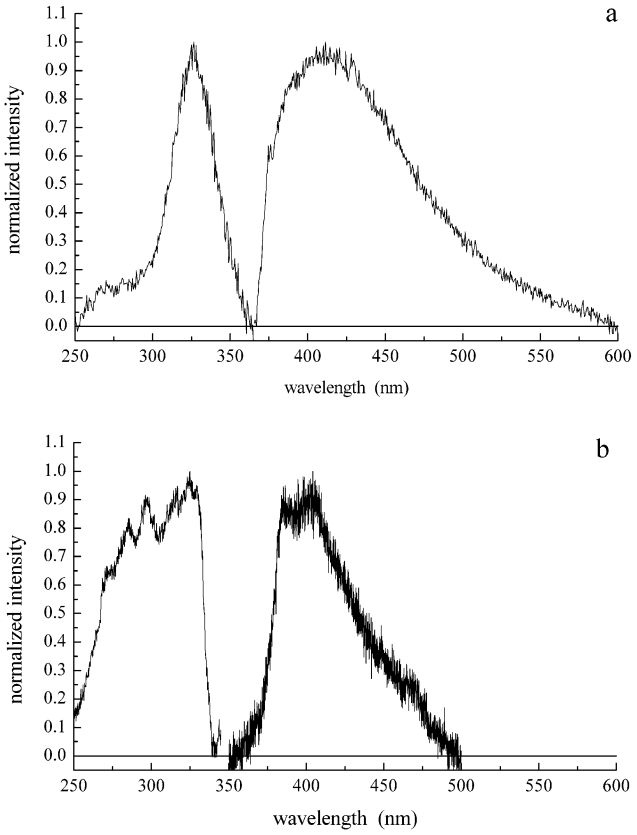

Figure 2. (a) Excitation and emission spectra of a single layer of 1-amidopyrene hexanoate bound to an ITO substrate. (b) Excitation and emission spectra of a single layer of 1-amidopyrene hexanoate bound to a SiO_x substrate. Excitation and emission spectra have been normalized for presentation purposes.

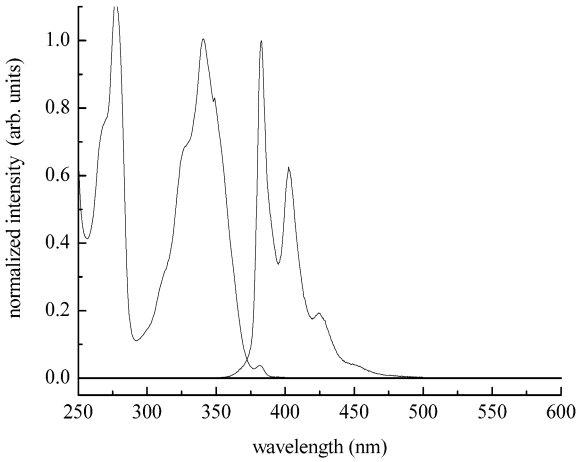

Figure 3. Normalized solution-phase absorption and emission spectra of 1-acetamidopyrene in 1-pentanol.

be reflective of differences in the extent of interaction between the chromophore and the substrate, but it is well established that the position of pyrene excimer bands depends sensitively on the geometric relationship between pyrene chromophores,[14] and it is reasonable to expect different adlayer structures for the quartz- and ITO-bound adlayers. For both the ITO- and quartz-bound pyrene chromophores, time-resolved data show that the chromophores are held relatively rigidly, and we describe our basis for this statement below.

Information about chromophore motion within the monolayers is obtained from time-domain experimental data by means of the anisotropy function, $R(t)$

$$R(t) = \frac{I_{||}(t) - I_{\perp}(t)}{I_{||}(t) + 2I_{\perp}(t)} \quad (1)$$

The quantities $I_{||}(t)$ and $I_{\perp}(t)$ are experimental time-resolved signal intensities for emission polarized parallel and perpendicular to the excitation polarization, respectively. The induced orientational anisotropy function is related to molecular motion. For chromophore motion in solution, where an initially anisotropic orientational distribution can achieve complete rerandomization, $R(t)$ tends to zero with increasing time, and the motional properties are typically described in the context of the modified Debye−Stokes−Einstein equation.[15,16] For reorientation on a substrate, the motional freedom of the (tethered) chromophore is restricted, and $R(t)$ approaches a nonzero value at long times.[17,18] The model used to interpret hindered motion assumes that the tethered chromophore sweeps out a conical volume in the interfacial layer, with the apex of the cone being the point of attachment to the substrate.[19,20] The value of $R(\infty)$ is related to the average angle that the chromophore makes with respect to the surface normal. For the reorientation of bound chromophores[19]

$$R(t) = R(\infty) + [R(0) - R(\infty)] \exp(-t/\tau) \quad (2)$$

The time constant τ is for the rerandomization of the chromophore to the extent possible, a quantity that is related to the size of the cone angle in which the chromophore is free to rotate. A value of $\tau = \infty$ corresponds to the chromophore being immobilized at or in the interfacial adlayer on the time scale of the experiment, with the recovered steady-state anisotropy being equal to $R(0)$. We observe $\tau = \infty$ for all of our interfacially bound chromophores, and this finding is consistent with the dominance of the aggregated form of pyrene on these samples. The quantity $R(0)$ is related to the angle δ between the excited and emitting transition moments[21]

$$R(0) = \frac{2}{5}P_2(\cos\delta) = \frac{1}{5}(3\cos^2\delta - 1) \quad (3)$$

where $P_2(\cos\delta)$ is the second-order Legendre polynomial in $\cos\delta$. In the work we report here, the value of δ is found to depend sensitively on the local environment of the chromophore.

We divide the chromophores used in this work (Figure 1) into two broad categories. In the first group are the molecules that are structural analogues of the surface-bound species but are not bonded to an interface. We use these molecules to understand the intrinsic properties of the tethered pyrene chromophore. The second category is the compound bound to the several interfaces that we discuss here. We consider the free chromophores first.

The optical response of pyrene is well understood,[3] and substituents on the pyrene ring system perturb its symmetry and thus the details of the vibronic coupling between the S_2 and S_1 manifolds. The value of $R(0)$ that we recover from solution-phase measurements varies according to the identity of the pyrene ring substituent, and we summarize these data in Table 1. The basis for this behavior is intramolecular interaction between the substituent terminal functionality and the pyrene ring system. For 1-aminopyrene, we find $R(0) = 0.15$ ($\delta = 40°$, Figure 4a), and for 1-acetamidopyrene, we measure $R(0) = 0.16$. The presence of these functionalities on the pyrene ring structure serves to mediate the S_2-S_1 vibronic coupling such that the measured angle between the excited and emitting transition dipole moment shifts by ∼50° relative to that of the native pyrene chromophore. For both of these substituents, the only means by which this effect can occur is by direct covalent connection to the chromophore. In terms of coupling to the ring system, the presence of aliphatic substituents beyond the amido functionality should not influence the pyrene π-system by through-bond interactions. Our measurement of $R(0) = -0.05$ ($\delta = 60°$, Figure 4b) for 1-amidopyrene hexanoic acid must

TABLE 1: Zero-Time Anisotropies, Corresponding Angles δ, and Reorientation and Fluorescence Lifetimes for Substituted Pyrenes in Solution

substituent	$R(0)$	δ^a (degrees)	τ_{OR} (ps)[b]	τ_{fl} (ns)
amino[b]	0.15 ± 0.01	40 ± 1	225	4.5
acetamido[c]	0.16 ± 0.01	39 ± 1	220	8.2
amidohexanoic acid[c]	-0.05 ± 0.01	60 ± 1	195	9.1
butanethiol[c]	-0.05 ± 0.01	60 ± 1	220	−

[a] Angles δ calculated from the $R(0)$ data using eq 3. [b] Reorientation time constant uncertainty is ±5%. [c] Data acquired in 1-pentanol. [d] Data from Karpovich, D. S.; Blanchard, G. J. *Langmuir* **1996**, *12*, 5522−5524. $R(0)$ value acquired in *n*-hexadecane solution.

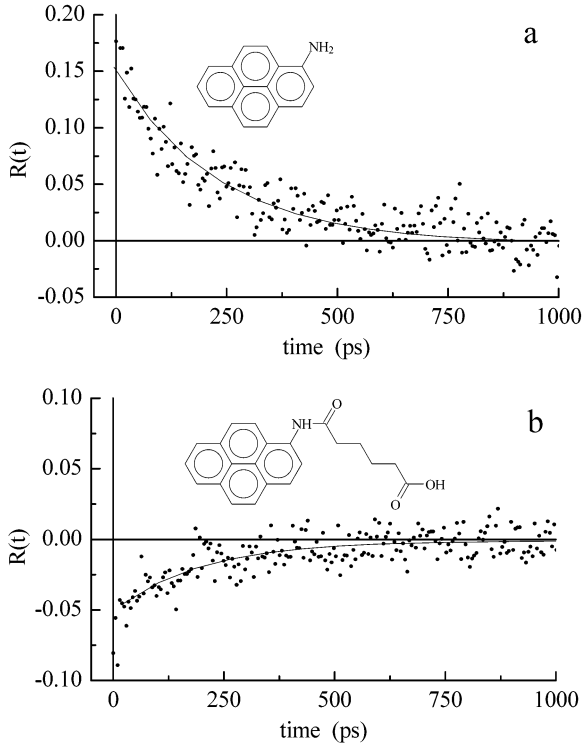

Figure 4. (a) Solution-phase anisotropy data for 1-aminopyrene in 1-pentanol. (b) Solution-phase anisotropy data for 1-amidopyrene hexanoic acid in 1-pentanol. The dots are experimental data points, and the solid line through the data is the best fit to a single-exponential decay function.

TABLE 2: Zero-Time Anisotropies and Corresponding Angles δ for Pyreneamidohexanoate Bound to Selected Substrates

substrate	$R(0)$	δ^a (degrees)
SiO_x	0.06 ± 0.05	49 ± 5
ITO	-0.08 ± 0.05	63 ± 6
Au	-0.14 ± 0.05	72 ± 9

[a] Angles δ calculated from the $R(0)$ data using eq 3.

thus be the result of sterically mediated intramolecular interactions between the terminal carboxylic acid functionality and the pyrene π-system. This finding is consistent with our earlier report of 1-pyrenebutanethiol exhibiting a negative zero-time anisotropy in solution[18] and underscores the sensitivity of S_2-S_1 vibronic coupling in the pyrene chromophore to its local environment. There is literature precedent for the pyrene chromophore interacting with alcohols by means of hydrogen bonding,[22-24] and this is likely the case here. We observe these effects in 1-pentanol, indicating that the intramolecular interactions can compete efficiently with intermolecular solvent−solute interactions. The fact that such intramolecular interactions are intrinsically asymmetric relative to the chromophore π-plane might also play a role in our observations.

The environmental sensitivity of vibronic coupling in substituted pyrenes is useful in probing the local environment of surface-bound species. From solution-phase measurements, we know that the addition of an amino or amido substituent to the pyrene ring shifts δ to $\sim$40° and that interactions between the pyrene ring and its local environment can move δ to $\sim$60°, with the strength of interaction presumably being related to the value of δ. With this information in hand, we consider the results obtained for surface-bound pyrene (Table 2).

The induced orientational anisotropy functions of 1-amidopyrene hexanoic acid tethered to the several interfaces are shown in Figures 5−7. Despite substantial changes in $R(0)$ with the identity of the substrate, we detect no motional relaxation behavior for any of the systems. For all interfaces, the pyrene chromophore is held rigidly on a nanosecond time scale. We note that some structural freedom might be present within the interface between its point of attachment to the substrate and the chromophore aggregates. Our IR data of the CH stretching-region for these interfaces suggest a liquidlike environment for the aliphatic chains according to the band positions in the CH stretching region (Figure 8, inset).[25] We note the presence of the aromatic CH stretching bands for the pyrene chromophore above 3000 cm^{-1}. The comparatively low intensity of these bands results from the low pyrene surface coverage (vide infra) and the orientation of the chromophore relative to the substrate. The rigid local environment of the chromophore is consistent with our steady-state spectroscopic results showing significant aggregation. The values of $R(0)$ reveal that the nature of the coupling between the chromophore and the substrate depends sensitively on the identity of the substrate. For the two conductive substrates, we recover negative anisotropy values, indicating $\delta > 55°$. This finding could, in principle, be the result of intermolecular interactions or substrate−chromophore interactions. We find that the same pyrene chromophore, when bound to a SiO_x substrate, exhibits a positive zero-time anisotropy, indicating that the negative $R(0)$ seen for pyrene on Au and ITO is the result of chromophore−substrate interactions. This is an induced dipole−induced dipole interaction, and the characteristic distances over which such interactions operate is longer than the chromophore−interface separation.[26-31] What remains to be determined is the information that can be extracted from the $R(0)$ data. We consider next the limitations on the information that can be obtained for these systems.

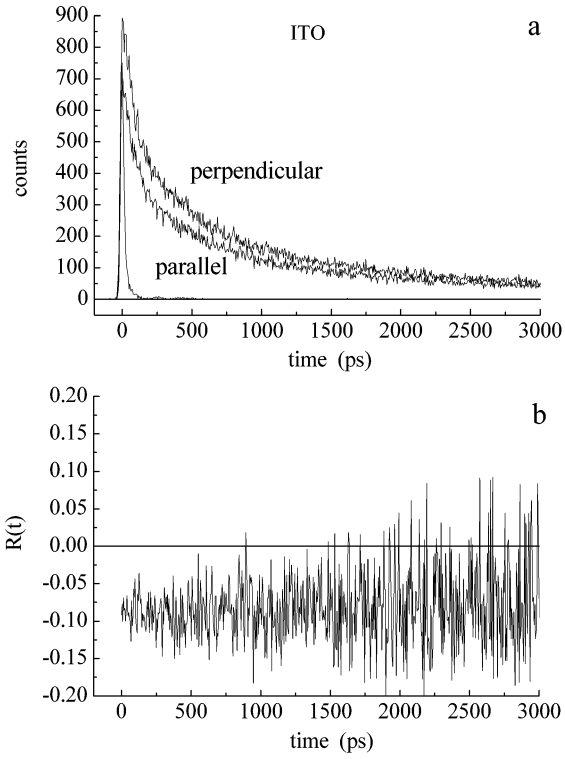

Figure 5. (a) Time-resolved intensity data for 1-amidopyrene hexanoate bound to an ITO substrate, with emission collection polarizations indicated. (b) Anisotropy function, $R(t)$, derived from the experimental data shown in panel a.

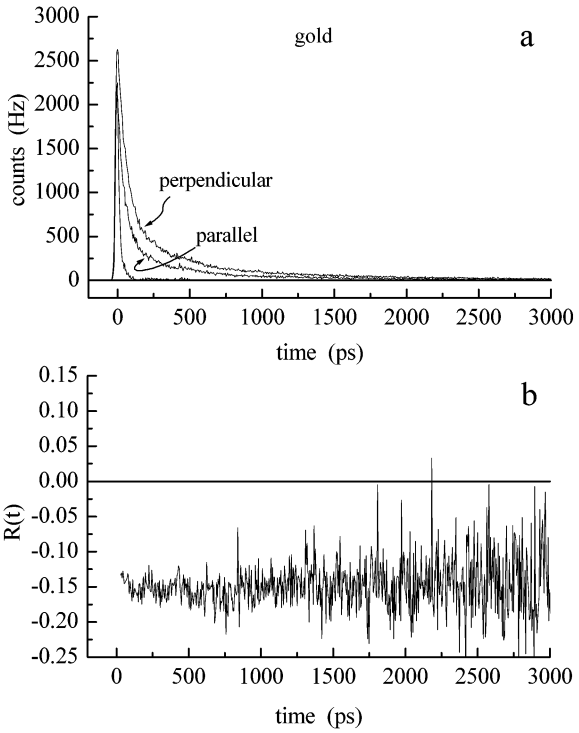

Figure 6. (a) Time-resolved intensity data for 1-amidopyrene hexanoate bound to a gold substrate by a layer of 6-mercapto-1-hexanol, with emission collection polarizations indicated. (b) Anisotropy function, $R(t)$, derived from the experimental data shown in panel a.

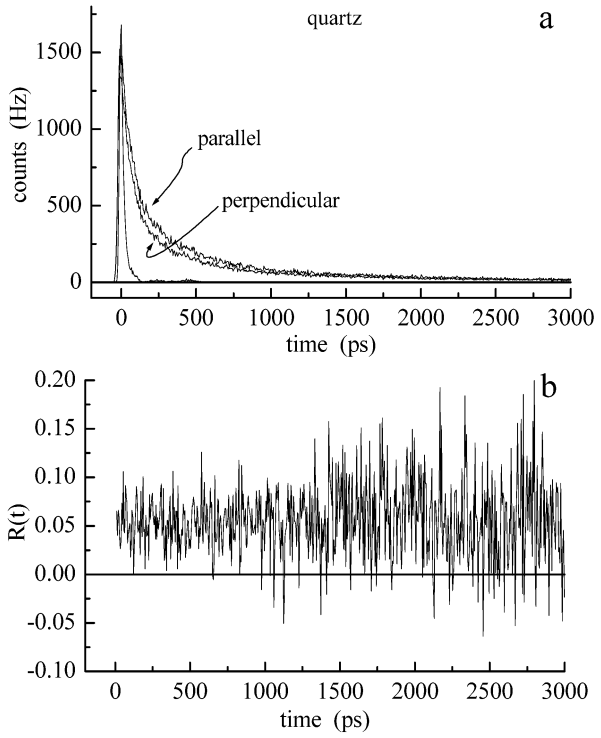

Figure 7. (a) Time-resolved intensity data for 1-amidopyrene hexanoate bound to a silica substrate, with emission collection polarizations indicated. (b) Anisotropy function, $R(t)$, derived from the experimental data shown in panel a.

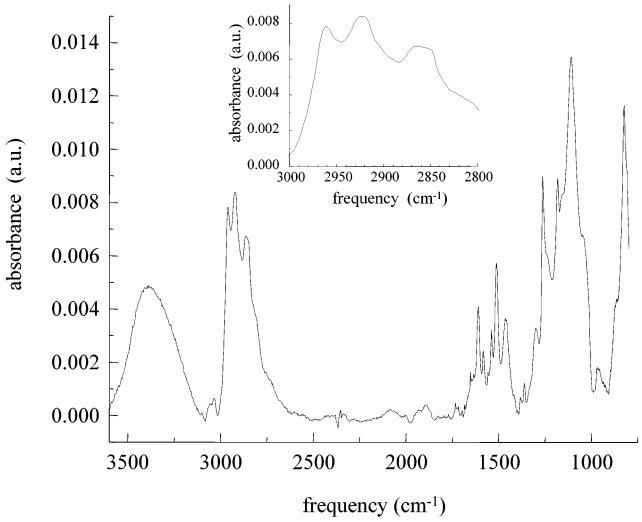

Figure 8. FTIR spectrum of a single layer of 1-amidopyrene hexanoate bound to a gold substrate. Inset: Aliphatic stretching region, showing band position and width consistent with substantial disorder within the adlayer.

Vibronic coupling between two electronic states can be described using a perturbation treatment, where the quantities of interest are the transition dipole moments, M, for the absorption and emission transitions.[3,32−36] It is the angle between these transition moments that is sensed by the quantity $R(0)$. Because of vibronic coupling, we do not measure simply $S_1 \leftrightarrow S_0$ transitions. Because of the substantial coupling of the excited states S_1 and S_2, the transitions that we access are more complex than simple $S_1^{v=v} \leftarrow S_0^{v=0}$ and $S_0^{v=v} \leftarrow S_1^{v=0}$ transitions seen for most other polycyclic aromatics. For molecules characterized by strong vibronic coupling, the transition moments M are given by[3,36]

$$M(S_1^{v=1} \leftarrow S_0^{v=0}) = -\sum_{S_2^{v=v}} \left\{ \left[1 + \frac{\hbar\omega_c}{\Delta E_0 + v\hbar\omega_v - \hbar\omega_c} \right] \times \left[\frac{\left\langle \theta_{S_2}^{v=v} \middle| \left\langle \varphi_{S_2} \middle| \frac{\partial H_e}{\partial q_c} \middle| \varphi_{S_1} \right\rangle \langle \theta_{S_0}^{v=c} | q_c | \theta_{S_1}^{v=c} \rangle \middle| \theta_{S_1}^{v=0} \right\rangle}{\Delta E_0 + v\hbar\omega_v} \right] \right\} R_{0-2} \langle \theta_{S_0}^{v=0} | \theta_{S_2}^{v=v} \rangle$$

$$M(S_0^{v=1} \leftarrow S_1^{v=0}) = -\sum_{S_2^{v=v}} \left\{ \left[1 - \frac{\hbar\omega_c}{\Delta E_0 + v\hbar\omega_v + \hbar\omega_c} \right] \times \left[\frac{\left\langle \theta_{S_2}^{v=v} \middle| \left\langle \varphi_{S_2} \middle| \frac{\partial H_e}{\partial q_c} \middle| \varphi_{S_1} \right\rangle \langle \theta_{S_0}^{v=c} | q_c | \theta_{S_1}^{v=c} \rangle \middle| \theta_{S_1}^{v=0} \right\rangle}{\Delta E_0 + v\hbar\omega_v} \right] \right\} R_{0-2} \langle \theta_{S_0}^{v=0} | \theta_{S_2}^{v=v} \rangle \quad (4)$$

The expressions for the transition dipole moments in eqs 4 are cast in terms of the electronic (φ) and vibrational (θ) wave functions for the relevant states, and the wave functions do not contain explicit information on the interaction of the pyrene molecule with its immediate environment. The extent to which vibronic coupling proceeds is determined by the interaction between the S_1 and S_2 manifolds along the coordinate q_c, which spans the transition moment axes. It is the operator $(\partial H_e/\partial q_c)$ that is sensitive to the pyrene immediate environment. For pyrene, q_c is taken as the coordinate that spans the orthogonal axes of the two electronic states, i.e., the b_{3g} vibrational modes.[37,38] This coupling is weak for the symmetric pyrene molecule, and thus small changes in $(\partial H_e/\partial q_c)$ can give rise to significant changes in the terms M. For substituted pyrenes, the presence of the substituent serves to couple the electronic transition moment axes, with the details of the coupling determining the angle of the effective transition moment for the absorbing transition(s) relative to the emitting ($S_0 \leftarrow S_1$) transition. This coupling is sufficiently strong for 1-aminopyrene to shift the measured angle between the transition moments by ~50° relative to that for pyrene. In addition to the intramolecular influence of ring substituents on the term $(\partial H_e/\partial q_c)$, there can also be intermolecular influences on $(\partial H_e/\partial q_c)$, with the extent of the effect being determined by the spatial relationship of the perturbation to the $S_1 \leftarrow S_0$ and $S_2 \leftarrow S_0$ transition moments. Because we do not know the Hamiltonian H_e for pyrene, we are not able to extract detailed structural information on local environment or chromophore−substrate interactions from our $R(0)$ data. We can determine whether intermolecular interactions create a perturbation to the pyrene transition moments that is comparable in magnitude to that seen for direct substitution on the ring system.

Despite the limitations indicated above, the zero-time anisotropy data for the bound chromophores suggest that the orientation of the pyrene π-system is nominally perpendicular to the substrate plane. We make this assertion on the basis of the argument that, if the interaction between the interface and both transition dipole moments were close to the same, as would be the case if the pyrene π-system were parallel to the substrate plane, we would see a small change in $R(0)$ compared to that

seen for 1-aminopyrene or 1-acetamidopyrene in solution. For the chromophore π-plane nominally perpendicular to the substrate plane, one of the transition dipole moments should project an image dipole onto the substrate more efficiently than the other, giving rise to a larger perturbation in the measured $R(0)$ value. This is the situation that we find experimentally, and we note that this condition is geometrically consistent with the formation of pyrene aggregates at the interface (Figure 2). If the pyrene chromophore π-plane were nominally parallel to the substrate plane, the pyrene chromophores would not be capable of forming face-on aggregates, which are known to be the favored structural conformation for pyrene excimers.[14]

Given the modest surface coverage obtained from the electrochemical data (1.7×10^{-11} mol cm^{-2}), it might be considered surprising to find the extent of pyrene aggregation that we report here. We assert that these two conditions are not mutually exclusive. Whereas the electrochemical data yield information on the overall surface concentration, such data are not informative in terms of the distribution of surface-bound species. Our evidence of aggregation on these surfaces is consistent with a nonuniform spatial distribution of adsorbates, and the electrochemical surface coverage data are not at odds with the spectroscopic data. Such aggregation phenomena have literature precedent for adlayers containing aromatic rings.[39−41] The formation of face-on aggregates, as seen from the steady-state data, points to the pyrene chromophore π-plane being nominally perpendicular to the substrate plane.

To verify that the orientation of the chromophore π-system relative to the ITO substrate serves to mediate the interactions that perturb the chromophore S_1-S_2 vibronic coupling, we created a monolayer structure that contains, in addition to the tethered pyrene chromophore, C_{12} aliphatic tails. The addition of the aliphatic moieties to the interfacial structure should change the orientation of the chromophores by virtue of steric interactions within the layer, consistent with our previous results on tethered pyrene bound to a gold substrate and confined within an alkanethiol SAM. We observed that, with the addition of the C_{12} aliphatic chains to the monolayer, the experimental value of $R(0)$ increased from -0.15 ($\delta = 73°$) to -0.20 ($\delta = 90°$). This finding is important in the sense that it demonstrates that the monolayer organization can and does influence how the tethered chromophore can interact with the substrate.

Conclusions

We have found that the steady-state spectroscopy of pyrene chromophores bound to several interfaces points to extensive aggregation. Time-resolved measurements indicate that there is substantial coupling between the pyrene chromophore and conductive (metallic, doped semiconductor) substrates. We understand this interaction in terms of vibronic coupling between the S_2 and S_1 states in the pyrene chromophore, and our anisotropy data demonstrate that the angle between the absorbing and emitting transition dipole moments depends on the details of this vibronic coupling and the orientation of the chromophore relative to the substrate plane. We anticipate that this information will find use in characterizing interfacial structures. More work will be required to relate the zero-time anisotropy data to the details of the perturbation that gives rise to the variations seen in δ.

Acknowledgment. We are grateful to the National Science Foundation for support of this work under Grant 0090864 and to NATO for support of P.K. under Grant CLG 977966.

References and Notes

(1) Krysinski, P.; Blanchard, G. J. *J. Electroanal. Chem.* **2003**, in review.
(2) Gritsch, S.; Nollert, P.; Jahnig, F.; Sackmann, E. *Langmuir* **1998**, *14*, 3118.
(3) Karpovich, D. S.; Blanchard, G. J. *J. Phys. Chem.* **1995**, *99*, 3951.
(4) Michota, A.; Kudelski, A.; Bukowska, J. *Surf. Sci.* **2002**, *502*, 214.
(5) Kudelski, A. *Surf. Sci.* **2002**, *502*, 219.
(6) Kudelski, A.; Hill, W. *Langmuir* **1999**, *15*, 3162.
(7) Krysinski, P.; Zebrowska, A.; Michota, A.; Bukowska, J.; Becucci, L.; Moncelli, M. R. *Langmuir* **2001**, *17*, 3852.
(8) Krysinski, P.; Zebrowska, A.; Palys, B.; Lotowski, Z. *J. Electrochem. Soc.* **2002**, *149*, E189.
(9) Dewitt, L.; Blanchard, G. J.; Legoff, E.; Benz, M. E.; Liao, J. H.; Kanatzidis, M. G. *J. Am. Chem. Soc.* **1993**, *115*, 12158.
(10) Saito, G.; Hirate, S.; Nishimura, K.; Yamochi, H. *J. Mater. Chem.* **2001**, *11*, 723.
(11) Oyama, M.; Higuchi, T.; Okazaki, S. *Electrochem. Commun.* **2001**, *3*, 363.
(12) Kerr, C. E.; Mitchell, C. D.; Headrick, J.; Eaton, B. E.; Netzel, T. L. *J. Phys. Chem. B* **2000**, *104*, 1637.
(13) Mitchell, C. D.; Netzel, T. L. *J. Phys. Chem. B* **2000**, *104*, 125.
(14) Michel-Beyerle, M. E.; Yakhot, V. *Chem. Phys. Lett.* **1977**, *49*, 463.
(15) Debye, P. *Polar Molecules*; Chemical Catalog Co.: New York, 1929.
(16) Perrin, F. *J. Phys. Radium* **1934**, *5*, 497.
(17) Horne, J. C.; Blanchard, G. J. *J. Am. Chem. Soc.* **1996**, *118*, 12788.
(18) Karpovich, D. S.; Blanchard, G. J. *Langmuir* **1996**, *12*, 5522.
(19) Lipari, G.; Szabo, A. *Biophys. J.* **1980**, *30*, 489.
(20) Szabo, A. *J. Chem. Phys.* **1984**, *81*, 150.
(21) Chuang, T. J.; Eisenthal, K. B. *J. Chem. Phys.* **1972**, *57*, 5094.
(22) Okada, T.; Karaki, I.; Mataga, N. *J. Am. Chem. Soc.* **1982**, *104*, 7191.
(23) Nakajima, A. *Bull. Chem. Soc. Jpn.* **1983**, *56*, 929.
(24) Fujii, T.; Shimizu, E.; Suzuki, S. *J. Chem. Soc., Faraday Trans.* **1988**, *84*, 4387.
(25) Porter, M. D.; Bright, T. B.; Allara, D. L.; Chidsey, C. E. D. *J. Am. Chem. Soc.* **1987**, *109*, 3559.
(26) Chance, R. R.; Prock, A.; Silbey, R. *Adv. Chem. Phys.* **1978**, *37*, 1.
(27) Avouris, P.; Schmeisser, D.; Demuth, J. E. *J. Chem. Phys.* **1983**, *79*, 488.
(28) Alivisatos, A. P.; Waldeck, D. H.; Harris, C. B. *J. Chem. Phys.* **1985**, *82*, 541.
(29) Kurczewska, H.; Bassler, H. *J. Lumin.* **1977**, *15*, 261.
(30) Persson, B. N. J.; Lang, N. D. *Phys. Rev. B* **1982**, *26*, 5409.
(31) Persson, B. N. J.; Avouris, P. *J. Chem. Phys.* **1983**, *79*, 5156.
(32) Salvi, P. R.; Castellucci, E.; Foggi, P.; Quacquarini. *Chem. Phys.* **1984**, *83*, 345.
(33) Cunningham, K.; Siebrand, W.; Williams, D. F.; Orlandi, G. *Chem. Phys. Lett.* **1973**, *20*, 496.
(34) Orlandi, G.; Siebrand, W. *Chem. Phys. Lett.* **1972**, *15*, 465.
(35) Orlandi, G.; Siebrand, W. *J. Chem. Phys.* **1973**, *58*, 4513.
(36) Geldof, P. A.; Rettschnick, R. P. H.; Hoytink, G. J. *Chem. Phys. Lett.* **1971**, *10*, 549.
(37) Mangle, E. A.; Topp, M. R. *J. Phys. Chem.* **1986**, *90*, 802.
(38) Bree, A.; Vilkos, V. V. B. *Spectrochim. Acta* **1971**, *27A*, 2333.
(39) Krysinski, P.; Jackowska, K.; Mazur, M.; Tagowska, M. *Electrochim. Acta* **2000**, *46*, 231.
(40) Mazur, M.; Krysinski, P. *Langmuir* **2001**, *17*, 7093.
(41) Turyan, I.; Mandler, D. *J. Am. Chem. Soc.* **1998**, *120*, 10733.